Synthesis and Characterization of Silver(II) Oxide

RIAZ QADEER, FIAZ AHMAD, SUMEERA IKRAM AND ARSHAD MUNIR
Pakistan Atomic Energy Commission, P.O. Box. No. 1331, Islamabad, Pakistan

(Received 18th August, 1998, revised 9th July, 1999)

Summary: Silver(II) oxide (AgO), an active material for batteries, was synthesized by oxidation of silver(I) nitrate in alkaline medium, and was characterized using various physico-chemical techniques for trace metal impurities, structure and thermal stabilities and various physical parameters. The results of analytical analyses involving x-ray fluorescence, atomic absorption and emission spectrometries reveal that the synthesized AgO has the purity >98% and contain Na, Fe, Ca, Cu, Mg, Zn, Si, Al, B etc. as traces. The structural and thermal investigations show that AgO has monoclinic structure and is stable upto 130°C, beyond that AgO decomposes into two stages; the first stage corresponds to the conversion of AgO to Ag_2O while the second stage is the indicative of Ag_2O to Ag conversion. The determined values of densities lie in the order of bulk density < tap density < true density, having surface area 0.307 m^2/g, average particle size 20.73 micron, pore volume 0.235 cm^3/g and porosity 57%.

Introduction

Silver oxide is considered to be a prime source for producing high energy zinc-silver oxide batteries. These batteries provide high current, more level voltage, greater ampere hour capacity per unit weight of battery and provide smooth discharge characteristics [1]. Two types of silver oxide i.e., monovalent silver oxide (Ag_2O) and divalent silver oxide (AgO) are being used as cathode materials. The zinc-silver oxide cell based on AgO has higher theoretical potential (1.8V) and high energy density (424 Wh/kg). In addition to these, AgO has low specific resistance and high conductivity as compared to Ag_2O. Specific resistance values of AgO and Ag_2O are in the range of 0.012-59.3 ohm-cm and 10^8 ohm-cm respectively[2-5]. The varied specific resistance values for AgO are due to the presence of impurities in AgO, where as high value of specific resistant for Ag_2O indicate the absence of mobile or unpaired electron in its lattice [6]. Due to these characteristics AgO is widely used as a cathode material in zinc-silver oxide batteries.

The cost of commercially available AgO is very high which increases the price of these batteries. In order to reduce the price, it was decided to synthesize the AgO in our laboratory. There are various ways to synthesize the AgO from acidic as well as from alkaline solutions. We have synthesized AgO by oxidation of silver(I) nitrate with potassium peroxydisulfate in an alkaline medium [7]. Details of this method and characterization of the prepared AgO using various analytical techniques are described in this communication.

Results and Discussion

The synthesized silver(II) oxide was black in colour and has a yield of 94%. Density values, given in Table-1, vary as: true density > tap density > bulk density, indicate maximum voids in the bulk density and least in the true density. It has a surface area value of 0.307 m^2/g indicating that the synthesized AgO is macroporous in nature.

Figure 1 shows the typical x-ray fluorescence spectrum of AgO, which constitutes of the following component:

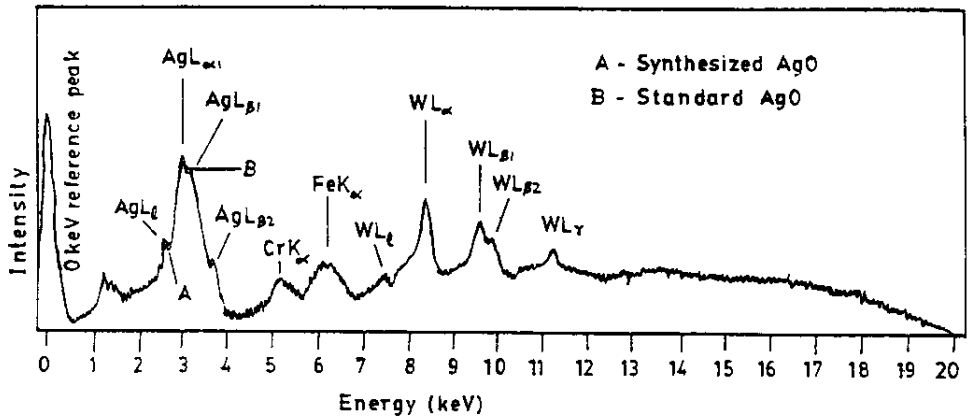

Fig. 1: EDXRF spectra of AgO.

Table-1: Determined values of different parameters of AgO

Surface area (N_2 adsorption	0.307 m^2/g
Bulk density	0.653 g/cm^3
Tap density	1.395 g/cm^3
True density	4.534 g/cm^3
Pore volume	0.235 cm^3/g
Porosity	57%
Pore area (Hg intrusion)	0.281 m^2/g
Average pore diameter	3.338 micron

1. Zero energy peak from the instrumental oscillator to monitor the reproducibility and the stability of the system as a whole. It also acts as a referance peak for the qualitative evolution of the system, which was within the limits of resolution and stability [8].
2. Resolved broad coherently scattered peak of $W_{l\alpha}$, W_{L1} and $W_{L\gamma}$ and unresolved $W_{\beta 1,\beta 2}$ peaks emitted from the anode target.
3. AgL_1, $AgL_{\alpha 1}$, $AgL_{\beta 1}$, $Agl_{\beta 2}$, peak emerged as secondary photons after photoelectric interaction of the primary x-ray beam with the sample specimen.
4. Peaks CrK_α and FeK_α are from the impurities present in the AgO which are added from the reactant materials.

It was also observed in Figure 1 that EDXRF profile of AgO matched fairly well with the EDXRF profile of a standard AgO (supplied by M/S Aldrich) obtained at identical conditions. The concentration of silver in AgO was measured by comparing the area of silver peak in the energy range of 2.7-3.6 keV with that of the area of standard and its concentration comes out to be 85.70%.

X-ray diffraction (XRD) data for AgO is presented in Table-2 show that AgO has a crystalline structure. Main diffraction lines appearing at 2.77, 2.41, 2.28 and 2.61 have relative intensities of 100, 88.2, 43 and 39.7 respectively. These and other smaller diffraction peaks coincide with the literature cited values for the compound [9]. The detailed studies of XRD data point towards a monoclinic crystal structure for the synthesized AgO.

Table-2: X-ray diffraction data of AgO

2 θ	d(A)	I/I_o
32.26	2.77	100
34.24	2.61	39
37.14	2.41	89
39.40	2.28	43
52.54	1.74	11
54.76	1.67	12
56.72	1.62	18
62.20	1.44	12
66.34	1.40	9
67.00	1.39	9
69.40	1.35	5
72.00	1.31	6
79.26	1.20	6
86.44	1.12	4
88.62	1.10	5
92.20	1.06	5

TG curve of AgO, Figure 2, shows that AgO is stable upto 130°C beyond which it decomposes to Ag_2O by elliminating half molecule of oxygen. AgO thus formed losses another half molecule of oxygen.

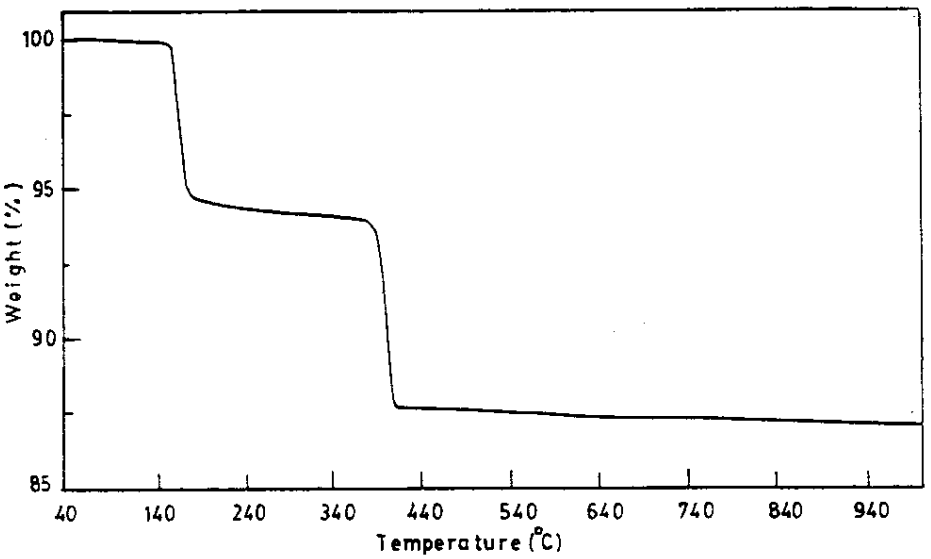

Fig. 2: TG pattern of AgO.

Ag_2O thus formed losses another half molecule of oxygen at temperature above 340°C resulting in the formation of Ag residue. Values of 5.83% (6.45%) and 6.375% (6.45%) weight loss are observed for the first and second stage decomposition respectively. These values are in agreement to the theoretically calculated values of weight loss for the respective stages and are given in parenthesis.

The plot of mercury intrusion and extrusion volume as a function of applied pressure for AgO, Figure 3, shows that there is a steep initial portion in the intrusion plot followed by a flat portion. As the applied pressure increases, there is again a sharp increase in intrusion volume of mercury and then the curve flattens reveals no further intrusion. The initial steep slop of the intrusion plot may be considered to be a consequence of penetration of mercury into the inter-particulate space [10]. Once the mercury has gained entry into the inter-particulate space, the slope of the curve flattened. As the pressure further increases, the intrusion occurs into pores of AgO and a stage come when no appreciable intrusion takes place with increasing pressure, indicating that little

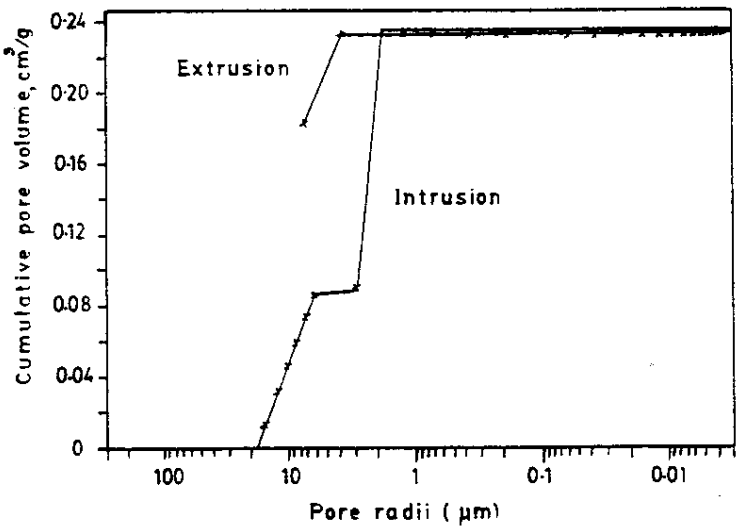

Fig. 3: Mercury intrusion/extrusion plots for AgO.

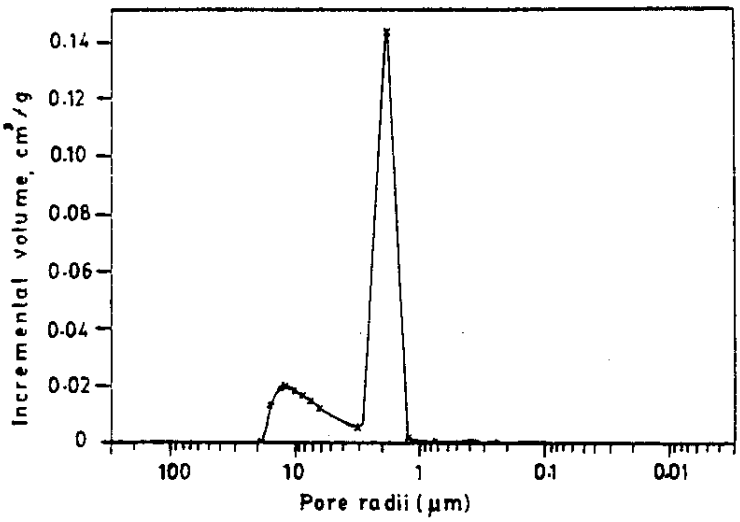

Fig. 4: Pore size distribution for AgO.

pore volume exist in the pores of radiii smaller than 1.8 micrometer. The extrusion curve shows that the mercury extrusion follow the same path as that of intrusion curve and after some time a small decrease in the intruded volume was observed, after which no extrusion was observed. It was found that after penetration and retraction, approximately 78% of mercury remained in the pores of AgO. This intrusion/extrusion behaviour indicates that AgO has pores of different shape. The matching patterns of intrusion and extrusion indicate the presence of cylindrical pores with constant cross-section [11]. Retention of 78% mercury within the pore indicates that the pore system deviate from simple cylindrical to ink-bottled pores [12] that are wider in the interior than exist. The mercury can not enter until pressure has risen to the value corresponding to the radius of the entrance capillary. On reducing the pressure, mercury does not leave the entrance of capillary due to the presence of pore potential which trap mercury once it intrudes into the pores [13].

The result of pore size distribution in which volume of mercury is transferred to pores as function of effective radii, r is given in Figure 4. This plot indicates two maxima occurring at effective radii 15 and 1.8 micron. The peak at 15 micron is due to the penetration of mercury in the inter-particle spaces. Height of the other peak shows that the contribution of pores of radius 1.8 micron is significant to the total pore volume. The pore surface area of AgO, determined by mercury intrusion, comes out to be 0.238 m^2/g. This value is quite similar to the surface area value determined by nitrogen adsorption which is 0.307 m^2/g. This indicates that AgO contains meso- and macropores. Values of other pore parameters are given in Table-1.

Experimental

Chemical used

The chemicals used in this study are: silver nitrate (locally prepared); potassium peroxydisulfate (98%, M/S E. Merck, item No. 5090); commercial sodium hydroxide.

Synthesis of AgO

The AgO was synthesized as per following reaction [14]:

$$4AgNO_3 + 2K_2S_2O_8 + 8NaOH \longrightarrow 4AgO + K_2SO_4 + 3Na_3SO_4 + 2NaNO_3 + 2KNO_3 + 4H_2O.$$

The flow sheet diagram for the synthesis of AgO is given in Figure 5 and details of the method can be seen in reference 14.

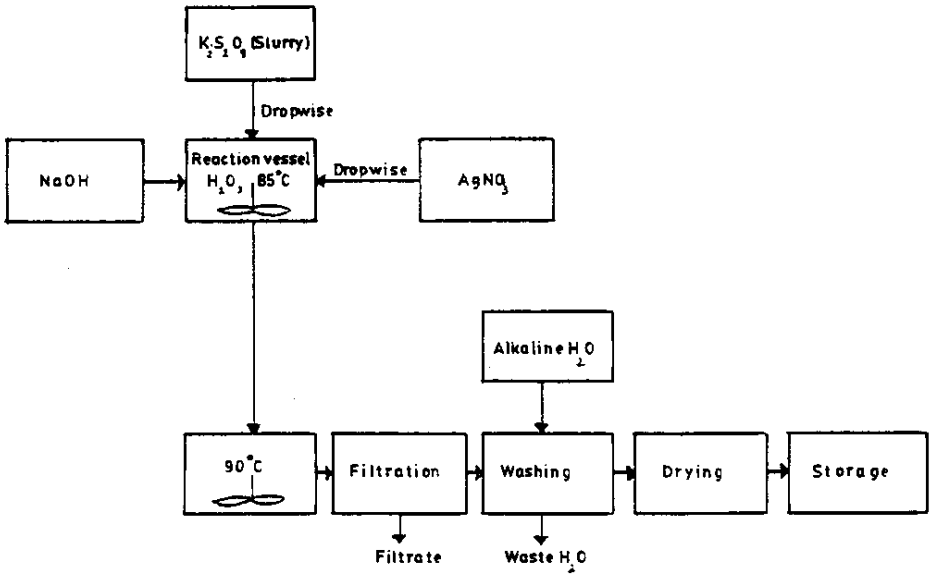

Fig. 5: Flow sheet diagram for the synthesis of AgO.

Characterization of synthesized AgO

Estimation of silver in AgO

Energy dispersive x-ray fluorescence (XR-500) from M/S Links Systems, U.K. was used to measure the concentration of silver in AgO. The system is equipped with 860 analyzer and 10 mm^2 x 3 mm deep Si(Li) detector with 155 eV resolution. The primary x-ray tube used in this study was K5012 SV with tungsten anode. Samples were prepared in a die [15] after loading known amount of sample powder backed by boric acid in a press (M/S Herzog) at 200 kNm^{-2} pressure. The pressed pellet was presented to spectrometer and x-ray spectrum was collected at voltage 20 kV and current 0.01 mA and is shown in Figure 1.

Estimation of trace metals impurities in AgO

The measurement of trace metal impurities in AgO was carried out by atomic absorption spectrometer and atomic emission spectrograph after dissolving the AgO in nitric acid solution. The description of the equipments and analytical conditions can be seen elsewhere [16,17]. The measured values of different impurities are given Table-2.

XRD studies of AgO

X-ray diffraction pattern of AgO was obtained with a Phillips PW 1060/70 diffractometer goniometer. The detector was argon filled proportional counter linked to a PW 1390 rate meter and channel analyzer. The radiation was CuK_α (1.5418 A) generated in a Phillips PW 1730 generator operated at 40kV and 30 mA. The x-ray diffraction data of AgO given in Table-3, was obtained by reflection from the surface of the sample spread on cellophane tape.

Table-3: Determined values of impurities in AgO

Metal	Conc. (ppm)	Technique
Na	88	AAS
Fe	70-90	AES
Ca	80	AAS
Cu	100-15	AES
Zn	25	AAS
Si	200	AES
Mg	traces	AES
Al	3-5	AES

AAS = Atomic absorption spectrometry
AES = Atomic emission spectrography

Estimation of surface area of synthesized AgO

Surface area of AgO powder was determined using Quantasorb Sorption system from M/S Quantachrome Corporation, N.Y. by a continuous flow method [18]. Nitrogen gas was adsorbed on the sample at liquid nitrogen temperature from a stream of nitrogen and helium (carrier gas). It was then desorbed and the liberated nitrogen measured by a thermal conductivity detector. Single point B.E.T.

equation [19] was used to determine surface area. Its measured value is given in Table-1.

Densities measurements

The bulk density and tap density of the synthesized AgO were measured according to the ASTM standard method No. D2854-70. Here, an empty cylinder of known volume was weighed, filled with AgO powder and weighed again. During the tap density measurement, the cylinder was tapped mechanically while being filled. The densities values obtained are given in Table-1.

True density of the AgO powder was determined using Quantasorb Sorption System. A known amount of AgO powder was filled into a special pycnometer cell which was volume calibrated. The cell was inserted into a cell holder of Quantasorb system and purged with nitrogen gas until constant electronics signals indicated complete filling of the cell. Another gas, helium was purged which replaced nitrogen from the cell. Volume of the nitrogen gas swept out of the cell was determined. True volume of powder in the cell is determined and the measured true density value of AgO is also given in Table-1.

Thermal studies of AgO

Thermal studies of AgO were carried out using TGA 7 thermogravimetric analyzer from M/S Perkin-Elmer, USA. A known amount of the sample was taken in platinum crucible and decomposition studies were carried out from 40°C to 1000°C at a heating rate of 20°C/min. This study was performed in an argon atmosphere. Typical TG curve obtained is given in Figure 2.

Pore size distribution studies of AgO

The mercury porosimetric study was performed to measure the pore volume, porosity and pore size distribution of AgO using AUTOPORE 9220 mercury porosimeter from M/S Micrometrics USA. Mercury was intruded into the pores of AgO as a function of pressure. The intrusion/extrusion curves for AgO are given in Figure 4 and the values of different pore parameters in Table-3.

Estimation of particle size

The particle size distribution of AgO was measured using Coulter Multisizer from M/S Coulter Electronics, U.K., after dispersing AgO in 1.0% NaCl solution, by wet sieving and sedimentation method. The particle size distribution curve is shown in Figure 6.

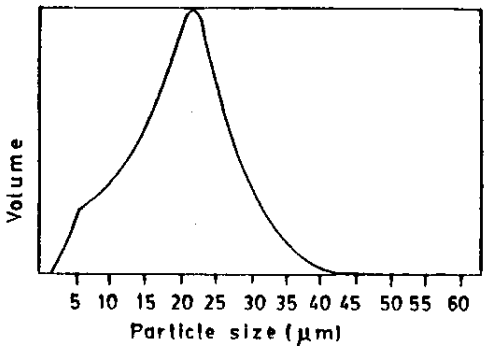

Fig. 6: Particle size distribution for AgO.

Conclusion

Two zinc-silver oxide single cells of 0.5 Ah capacity were prepared using synthesized and imported AgO as cathode material. The anode was prepared from electrolytic zinc powder. The details of the fabrication and the discharge of the cells will be published in a separate communication. These cells were discharged\using KOH as an electrolyte at 1A constant current. Results, given in Table-4, indicate that the performance of the synthesized AgO is slightly better than the battery's grade imported AgO.

Table-4: Discharged characteristics of single zinc-silver oxide cells

Parameter	Cell # 1	Cell # 2
Open circuit voltage	1.58 V	1.56 V
Constant current load	1.0 A	1.0 A
On-load voltage	1.38 V	1.34 V
Discharged time	40 mins.	37 mins
Cell capacity	0.66 Ah	0.61 Ah

The cost of the AgO synthesized in our laboratory was calculated as Rs. 2000.00 per 100 g. This cost include the raw materials cost and the over and above expenditures. The price for the same imported materials varies from Rs. 7500.00 to Rs. 14,500.00 per 100 g.

On the basis of the above observations, it is concluded that the activity of battery grade AgO synthesized in our laboratory is better than the activity of the imported one and is also economical.

enable us to reduce the price of the zinc-silver oxide batteries.

Acknowledgements

Authors are thankful to Dr. Samar Mubarakmand, S.I., H.I., Member Technical (P.A.E.C.) and Mr. Irfan Burney, S.I., Director for their cooperation and encouragement during this work.

References

1. T.R. Crompton, Battery Reference Book, Pub., Butterworth, London, Section 5 (1990).
2. M.LcBlanc and H. Sachse, *Physik Z*, **32**, 887 (1931).
3. P. Jones and H.R. Thirsk, *Trans Faraday Soc.*, **50**, 732 (1954).
4. A.B. Neiding and I.A. Kazarnovsko, *Dokl. Akad. Nauk. SSSR*, **78**, 713 (1951).
5. A. Tvarusko, *J. Electrochem. Soc.*, **115**, 1105 (1968).
6. T.P. Dirkse, In Zinc-Silver Oxide Batteris, eds. A. Fleischer and J. Lander, Pub. John Wiley and Sons Inc., New York, p. 102 (1971).
7. De Boer and Van Ormondt, *Chem. Abstract.*, **41**, 1401b (1947).
8. M. Afzal, J. Hanif, M. Saleem, I. Hanif and R. Ahmed, *J. Radioanal. Nucl. Chem. Articles*, **152**, 251 (1991).
9. JCPSD Card No. 22-472 pub. Joint Committee on Powder Diffraction and Standards.
10. C.H. Giles, D.C. Havard W. McMillan, T. Smith and R. Wilson, In Characterization of Porous Solids, eds. SJ. Gregg, K.S.W. Sing and H.F. Stoeckli, pub. London Society of Chemical Industry, 267 (1979).
11. M. Afzal, F. Mahmood and M. Saleem, *J. Chem. Soc. Pak.*, **15**, 100 (1993).
12. P.H. Emmett, *Chem. Rev.*, **43**, 69 (1948).
13. M.M. Dubinin, M.M. Vishnyakova, E.A. Leontev, V.M. Lukyanovich and A.I. Sarachov, *Zhur. Fiz. Kim.*, **34**, 2019 (1960).
14. R.N. Hammer and J. Kleinberg, *Inorg. Synthesis*, **4** 12 (1953).
15. I. Hanif, J. Hanif and M.Z. Iqbal, *The Nucleus*, **32**, 125 (1995).
16. R. Qadeer, Ph.D Thesis, Quaid-i-Azam University, Islamabad, Pakistan, 46 (1993).
17. R. Hussain, M. Ishaque, S. Hussain and D. Mohammad, *Sci. Technol. Dev.*, **10**, 30 (1991).
18. F.M. Nelson and F.T. Eggertsen, *Anal. Chem.*, **30**, 1387 (1958).
19. S. Lowell, Introduction to Powder Surface Area Measurement, Pub. John Willey & Sons, New York, p. 25 (1979).